

PACS numbers: 42.65.Re; 42.65.Sf
DOI: 10.1070/QE2007v037n06ABEH013440

Interaction of few-cycle laser pulses in an isotropic nonlinear medium

D.L. Oganesyan, A.O. Vardanyan

***Abstract*. The interaction of few-cycle laser pulses propagating in an isotropic nonlinear medium is studied theoretically. A system of nonlinear Maxwell's equations is integrated numerically with respect to time by the finite difference method. The interaction of mutually orthogonal linearly polarised 0.81-μm, 10-fs pulses is considered. Both the instant Kerr polarisation response and Raman inertial response of the medium in the nonlinear part of the medium are taken into account. The spectral shift of the probe pulse caused by the cross-action of the reference pulse is studied. The spectra of the interacting pulses are studied for different time delays between them and the shifts of these spectra are obtained as a function of the time delay.**

Keywords: *femtosecond laser pulse, nonstationary stimulated Raman scattering, spectral shift, finite difference method.*

1. Introduction

Nonstationary stimulated Raman scattering (SRS) of few-cycle femtosecond laser pulses (FLPs) opens up fundamentally new possibilities for studying elementary excitations in condensed media. The use of FLPs of duration τ_0 shorter or equal to the period T_m of molecular vibrations in a medium

$$\tau_0 \leqslant T_m = \frac{2\pi}{\Omega_m}, \tag{1}$$

where Ω_m is the frequency of molecular vibrations of the medium, allows one to study the vibrational dynamics of molecules. For example, the Stokes frequency shift in fused silica is $\Omega_m/(2\pi) = 13.05$ THz and the Raman line width is $\Delta\Omega_m/(2\pi) \approx 31$ THz. Therefore, condition (1) is fulfilled for a Gaussian femtosecond pulse of duration $\tau_0 = 10$ fs and the spectral width 44 THz.

The physics of interaction of few-cycle FLPs with a medium involves a number of specific features. When inequality (1) is valid, the spectral width of the exciting pulse exceeds the Stokes shift:

$$\Delta\omega_0 \approx \tau_0^{-1} \geqslant \Omega_m. \tag{2}$$

For this reason, there is no need to use biharmonic pumping to excite molecular vibrations and a Raman resonance can be excited by a few-cycle FLP because the Stokes component shifted by the molecular vibrational frequency is contained in the spectrum of the pulse itself. In this case, SRS represents a peculiar Raman self-action. The excitation of molecular vibrations leads to the redistribution of energy in the FLP spectrum, resulting in the red shift of the pulse spectrum [1, 2].

The use of few-cycle FLPs also permits the control of the amplitude and phase of molecular vibrations. Of interest is also the interaction of such FLPs in an isotropic nonlinear medium (from the point of view of controlling the amplitude and phase of molecular vibrations of the medium). For example, as shown in [2], if a medium is irradiated by two femtosecond pulses, the second, probe, pulse being delayed by time Δt with respect to the first, reference, pulse, then depending on Δt, the second pulse can enhance or weaken molecular vibrations excited by the first pulse and change their phase. It is obvious that in this case the energy distribution in the probe pulse spectrum will be also a function of the time delay between pulses. Namely, depending on Δt, the spectral shift of the probe pulse will be determined by either only the Raman self-action of the probe pulse itself or the Raman self-action of the probe pulse and the cross-action of the reference pulse on the probe pulse. The latter will result in the additional red shift of the probe pulse spectrum [3]. It is obvious that, if the time delay Δt greatly exceeds the period of molecular vibrations T_m, the cross-action of the reference pulse on the probe pulse can be neglected.

The nonlinear interaction of the probe (Stokes) pulse with the pump pulse propagating in fused silica was theoretically studied in the slowly varying amplitude (SVA) approximation in [3]. The dependences of the spectral shift of the Stokes pulse on the medium length were obtained taking into account the cross-action of the pump pulse on the Stokes pulse. The Stokes and pump pulse durations were longer than or equal to 100 fs.

It is shown in [4] that, when a subpicosecond soliton with the central wavelength located in the region of anomalous group-velocity dispersion propagates in fused silica, the red shift of the pulse spectrum caused by Raman self-action is

D.L. Oganesyan Yerevan State University, ul. A. Manukyana 1, 375049 Yerevan, Armenia; e-mail: davh1@netsys.am, dhovhannisyan@yahoo.com;
A.O. Vardanyan Yerevan Research Institute for Optophysical Measurements, ul. A. Sarkisyana 5a, 375031 Yerevan, Armenia

Received 27 September 2006; revision received 12 April 2007
Kvantovaya Elektronika **37** (6) 554 – 560 (2007)
Translated by M.N. Sapozhnikov

inversely proportional to the fourth power of the pulse duration and directly proportional to its energy. According to the results obtained in [5], when a femtosecond pulse with the central wavelength located in the region of normal group-velocity dispersion propagates in fused silica, the red shift of the pulse spectrum is inversely proportional to the third power of the pulse duration and directly proportional to its energy.

Note that the theoretically correct description of the propagation of few-cycle laser pulses in an isotropic nonlinear medium is of current interest because the duration of such pulses is shorter than the period of molecular vibrations of the medium and the pulse response of the medium contains the most complete information on relaxation processes proceeding in it.

The nonlinear propagation of a femtosecond pulse was studied in papers [3–5] within the framework of the SVA approximation. However, for few-cycle laser pulses considered here, the usual concept of the pulse envelope in invalid. For this reason, a new approximation, which is more correct than the SVA approximation, was developed recently to describe the propagation of pulses consisting of no more than ten field cycles (which are called few-cycle pulses). The equations describing the evolution of the electric field of a pulse rather than of its envelope are derived and analysed within the framework of this approximation [6, 7].

At the same time, great recent interest in the use of finite difference methods of direct numerical integration with respect to time for studying femtosecond processes is explained by the fact that such an approach allows one to simulate quite simply a number of phenomena in the nonlinear optics of few-cycle laser pulses based only on information about the optical properties of a medium itself. This model is quite universal and permits the simulation of the simplest case of free space as well as different combinations of nonlinear and dispersion media [8–16].

In this paper, we studied theoretically the interaction of few-cycle laser pulses propagating in fused silica. A system of nonlinear Maxwell's equations was integrated numerically with respect to time by the finite difference method. Linearly polarised pulses with equal central frequencies and mutually orthogonal polarisations were considered. The evolution of the spectra of the interacting pulses was studied for different time delays Δt between them and the dependences of the shift of these spectra on Δt were obtained. The time delay between the interacting pulses was varied in calculations from -20 to 40 fs.

2. Mathematical model of the nonlinear interaction of linearly polarised FLPs with mutually orthogonal polarisations

We will describe the propagation of orthogonally polarised plane wave packets in an isotropic nonlinear dispersion medium within the framework of the system of Maxwell's equations for the strengths of electric (E_x, E_y) and magnetic (H_y, H_x) fields

$$\frac{\partial D_y}{\partial t} = \frac{\partial H_x}{\partial z}, \quad \frac{\partial H_x}{\partial t} = \frac{1}{\mu_0}\frac{\partial E_y}{\partial z}, \tag{3}$$

$$\frac{\partial D_x}{\partial t} = -\frac{\partial H_y}{\partial z}, \quad \frac{\partial H_y}{\partial t} = -\frac{1}{\mu_0}\frac{\partial E_x}{\partial z}. \tag{4}$$

The relation between the electric field strengths E_x, E_y and electric inductions D_x, D_y is determined from the constitutive equation in which the linear dispersion of the medium and the Kerr and Raman nonlinearities are consistently taken into account:

$$D_y = \varepsilon_0 E_y + P_{y\mathrm{L}} + P_{y\mathrm{NL}}, \tag{5}$$

$$D_x = \varepsilon_0 E_x + P_{x\mathrm{L}} + P_{x\mathrm{NL}}, \tag{6}$$

where $P_{y\mathrm{L}}$, $P_{x\mathrm{L}}$ and $P_{y\mathrm{NL}}$, $P_{x\mathrm{NL}}$ are the linear and nonlinear parts of the polarisability of the medium, respectively.

As an isotropic nonlinear dispersion medium, we consider fused silica used for fabricating single-mode fibres for communication lines.

It is known that the linear susceptibility $\chi^{(1)}$ of fused silica is described by the expression [17]

$$\chi^{(1)}(\omega) = n^2(\omega) - 1 = \sum_{i=1}^{3} \frac{b_i \omega_i^2}{\omega_i^2 - \omega^2}, \tag{7}$$

where $b_1 = 0.6961663$; $b_2 = 0.4079426$; $b_3 = 0.897479$; $\lambda_1 = 0.0684043$ μm; $\lambda_2 = 0.1162414$ μm; $\lambda_3 = 9.896161$ μm; and $\lambda_i = 2\pi c/\omega_i$.

According to (7), the linear response of the medium is described by the expressions

$$P_{x\mathrm{L},\,y\mathrm{L}}(\omega) = \varepsilon_0 \sum_{i=1}^{3} \frac{b_i \omega_i^2}{\omega_i^2 - \omega^2} E_{x,y}(\omega)$$

$$= P_{1x\mathrm{L},\,1y\mathrm{L}}(\omega) + P_{2x\mathrm{L},\,2y\mathrm{L}}(\omega) + P_{3x\mathrm{L},\,3y\mathrm{L}}(\omega). \tag{8}$$

The system of equations (8) can be represented by the system of differential equations

$$\frac{1}{\omega_i^2}\frac{\partial^2 P_{iy\mathrm{L}}}{\partial t^2} + P_{iy\mathrm{L}} = \varepsilon_0 b_i E_y(t), \tag{9}$$

$$\frac{1}{\omega_i^2}\frac{\partial^2 P_{ix\mathrm{L}}}{\partial t^2} + P_{ix\mathrm{L}} = \varepsilon_0 b_i E_x(t), \tag{10}$$

where $i = 1, 2, 3$.

Equations (9) and (10) describe the linear dispersion properties of the medium in the transparency band according to the classical Lorentz model.

Taking into account the Kerr and Raman nonlinearities, the nonlinear response of the medium can be represented in the form

$$P_{x\mathrm{NL}}(t) = \varepsilon_0 E_x(t) \int_{-\infty}^{t} \chi^{(3)}(t-\tau) E_x^2(\tau)\mathrm{d}\tau$$

$$+ \varepsilon_0 E_x(t) \int_{-\infty}^{t} \chi^{(3)}(t-\tau) E_y^2(\tau)\mathrm{d}\tau, \tag{11}$$

$$P_{y\mathrm{NL}}(t) = \varepsilon_0 E_y(t) \int_{-\infty}^{t} \chi^{(3)}(t-\tau) E_y^2(\tau)\mathrm{d}\tau$$

$$+ \varepsilon_0 E_y(t) \int_{-\infty}^{t} \chi^{(3)}(t-\tau) E_x^2(\tau)\mathrm{d}\tau, \tag{12}$$

where $\chi^{(3)}(t) = \chi_0^{(3)} g(t)$; $\chi_0^{(3)}$ is the Kerr nonlinearity coefficient;

$$g(t) = \alpha\delta(t) + (1-\alpha)g_{\mathrm{R}}(t); \tag{13}$$

$$g_{\mathrm{R}}(t) = \frac{\tau_1^2+\tau_2^2}{\tau_1\tau_2^2}\exp\left(-\frac{t}{\tau_2}\right)\sin\frac{t}{\tau_1}; \tag{14}$$

$\alpha = 0.7$ is the dimensionless coefficient determining the contribution of the Kerr nonlinearity to the total nonlinear contribution to the nonlinear polarisation of the medium; $\delta(t)$ is the Dirac delta function; $g_{\mathrm{R}}(t)$ is the Raman response of the medium; $\tau_1 = 12.2$ fs; and $\tau_2 = 32$ fs.

The first terms in the right-hand side of Eqns (11) and (12) describe the self-action of pulses, while the second terms describe their cross-action. According to (11) and (12), the nonlinear response of the medium caused only by the Kerr inertialless nonlinearity can be written in the form

$$P_{x\mathrm{KNL}}(t) = \alpha\varepsilon_0\chi_0^{(3)}E_x^3(t) + \alpha\varepsilon_0\chi_0^{(3)}E_x(t)E_y^2(t), \tag{15a}$$

$$P_{y\mathrm{KNL}}(t) = \alpha\varepsilon_0\chi_0^{(3)}E_y^3(t) + \alpha\varepsilon_0\chi_0^{(3)}E_y(t)E_x^2(t), \tag{15b}$$

while the nonlinear response of the medium caused only by the Raman inertialless nonlinearity is described by the expressions

$$P_{x\mathrm{RNL}}(t) = \varepsilon_0(1-\alpha)\chi_0^{(3)}E_x(t) \times\left[\int_{-\infty}^{t} g_{\mathrm{R}}(t-\tau)E_x^2(\tau)\mathrm{d}\tau + \int_{-\infty}^{t} g_{\mathrm{R}}(t-\tau)E_y^2(\tau)\mathrm{d}\tau\right], \tag{16a}$$

$$P_{y\mathrm{RNL}}(t) = \varepsilon_0(1-\alpha)\chi_0^{(3)}E_y(t) \times\left[\int_{-\infty}^{t} g_{\mathrm{R}}(t-\tau)E_y^2(\tau)\mathrm{d}\tau + \int_{-\infty}^{t} g_{\mathrm{R}}(t-\tau)E_x^2(\tau)\mathrm{d}\tau\right]. \tag{16b}$$

Let us introduce new additional functions $S_x(t)$ and $S_y(t)$ corresponding to the convolution integrals

$$S_x(t) = \int_{-\infty}^{t} g_{\mathrm{R}}(t-\tau)E_x^2(\tau)\mathrm{d}\tau, \qquad S_y(t) = \int_{-\infty}^{t} g_{\mathrm{R}}(t-\tau)E_y^2(\tau)\mathrm{d}\tau, \tag{17}$$

whose Fourier transforms can be written in the form

$$S_x(\omega) = g_{\mathrm{R}}(\omega)\mathscr{F}\left[E_x^2(t)\right], \quad S_y(\omega) = g_{\mathrm{R}}(\omega)\mathscr{F}\left[E_y^2(t)\right], \tag{18}$$

where

$$\mathscr{F}\left[E_{x,y}^2(t)\right] = \int_{-\infty}^{\infty} E_{x,y}^2(t)\exp(-\mathrm{j}\omega t)\mathrm{d}t;$$

$$g_{\mathrm{R}}(\omega) = \frac{\omega_{\mathrm{R}}^2}{\omega_{\mathrm{R}}^2 + \mathrm{j}2\omega\delta_{\mathrm{R}} - \omega^2}; \tag{19}$$

$$\omega_{\mathrm{R}} = \left(\frac{\tau_1^2+\tau_2^2}{\tau_1^2\tau_2^2}\right)^{1/2}; \quad \delta_{\mathrm{R}} = \frac{1}{\tau_2}; \tag{20}$$

$1/(2\pi\tau_1) = 13.05$ THz is the optical phonon frequency of the medium; and τ_2 is the average phonon lifetime.

Therefore, the Fourier transforms of the functions $S_x(t)$ and $S_y(t)$ can be written in the form

$$S_x(\omega) = \frac{\omega_{\mathrm{R}}^2}{\omega_{\mathrm{R}}^2 + 2\mathrm{j}\omega\delta_{\mathrm{R}} - \omega^2}\mathscr{F}\left[E_x^2(t)\right], \qquad S_y(\omega) = \frac{\omega_{\mathrm{R}}^2}{\omega_{\mathrm{R}}^2 + 2\mathrm{j}\omega\delta_{\mathrm{R}} - \omega^2}\mathscr{F}\left[E_y^2(t)\right]. \tag{21}$$

One can see from Eqns (21) that the phonon response of the medium satisfies the differential equations

$$\omega_{\mathrm{R}}^2 S_x(t) + 2\delta_{\mathrm{R}}\frac{\partial S_x(t)}{\partial t} + \frac{\partial^2 S_x(t)}{\partial t^2} = \omega_{\mathrm{R}}^2 E_x^2(t), \qquad \omega_{\mathrm{R}}^2 S_y(t) + 2\delta_{\mathrm{R}}\frac{\partial S_y(t)}{\partial t} + \frac{\partial^2 S_y(t)}{\partial t^2} = \omega_{\mathrm{R}}^2 E_y^2(t), \tag{22}$$

which describe the oscillator SRS model of Platonenko–Khokhlov [18].

Thus, taking (15), (16), and (17) into account, the nonlinear polarisation of the medium can be represented in the form

$$\begin{aligned} P_{x\mathrm{NL}}(t) &= E_x(t)\left[\varepsilon_0\alpha\chi_0^{(3)}E_x^2(t) + (1-\alpha)\varepsilon_0\chi_0^{(3)}S_x(t)\right] \\ &\quad + E_x(t)\left[\varepsilon_0\alpha\chi_0^{(3)}E_y^2(t) + (1-\alpha)\varepsilon_0\chi_0^{(3)}S_y(t)\right], \\ P_{y\mathrm{NL}}(t) &= E_y(t)\left[\varepsilon_0\alpha\chi_0^{(3)}E_y^2(t) + (1-\alpha)\varepsilon_0\chi_0^{(3)}S_y(t)\right] \\ &\quad + E_y(t)\left[\varepsilon_0\alpha\chi_0^{(3)}E_x^2(t) + (1-\alpha)\varepsilon_0\chi_0^{(3)}S_x(t)\right]. \end{aligned} \tag{23}$$

Taking (5), (6), (10), and (23) into account, the electric inductions D_y and D_x can be written in the form

$$D_y = \varepsilon_0\left[E_y + \alpha\chi_0^{(3)}E_y^3 + \alpha\chi_0^{(3)}E_x^2E_y\right] + \sum_{i=1}^{3}P_{iy\mathrm{L}} + (1-\alpha)\varepsilon_0\chi_0^{(3)}E_yG_y + (1-\alpha)\varepsilon_0\chi_0^{(3)}E_yG_x, \tag{24}$$

$$D_x = \varepsilon_0\left[E_x + \alpha\chi_0^{(3)}E_x^3 + \alpha\chi_0^{(3)}E_y^2E_x\right] + \sum_{i=1}^{3}P_{ix\mathrm{L}} + (1-\alpha)\varepsilon_0\chi_0^{(3)}E_xG_x + (1-\alpha)\varepsilon_0\chi_0^{(3)}E_xG_y. \tag{25}$$

We used the above-described classical model of the interaction of a high-power femtosecond laser pulse (i.e. when $E_y = 0$, $E_x \neq 0$ or $E_y \neq 0$, $E_x = 0$) with the isotropic dispersion nonlinear medium to describe the self-action of radiation and Raman scattering [19]. This model was used in [12] to describe the nonlinear dynamics of a femtosecond optical soliton.

In this paper, we adapted this model to apply for studying the nonlinear interaction of linearly polarised FLPs with mutually orthogonal polarisations and identical carrier frequencies in an isotropic dispersion nonlinear medium.

3. Numerical scheme for integrating a system of nonlinear Maxwell's equations

The main problem of realisation of numerical schemes for integrating nonlinear Maxwell's equations is the algorithm stability. We used here the modified finite difference scheme for solving nonlinear Maxwell's equations proposed in [12].

As shown in [12], the modified finite difference scheme has a high stability and its dispersion parameters are two orders of magnitude higher than those reported in [9–11], and the consideration of nonlinearity does not cause the divergence of the numerical scheme. We used this numerical scheme to describe the interaction of FLPs with an isotropic dispersion nonlinear medium [19].

To simulate numerically processes described by Eqns (3), (4), (9), (10), (23)–(25), we will pass to the network functions for the fields $\boldsymbol{E}$ and $\boldsymbol{H}$, the electric induction $\boldsymbol{D}$, the linear and nonlinear responses P_{L} and P_{NL}, and functions S_x and S_y for which networks are specified over the coordinate $k\Delta z$ and time $n\Delta t$. The step Δz of the spatial network was set equal to 15 nm, the time step, determined by the Courant condition $\Delta t = \Delta z/2c$, was equal to 0.025 fs. For such a time step, the dispersion of the linear part of the scheme was maximally close to the Lorentzian dispersion of the medium. The difference scheme is an explicit scheme of the second-order accuracy in z. The values of the magnetic field are specified between the network nodes along the coordinate z and in the intermediate layer in time.

The numerical integration was performed for the normalised quantities

$$\bar{E}_x = \sqrt{\frac{\varepsilon_0}{\mu_0}}E_x, \quad \bar{D}_x = \sqrt{\frac{1}{\varepsilon_0\mu_0}}D_x, \quad \bar{H}_y = H_y,$$

$$\bar{P}_{x\mathrm{L}} = \frac{1}{\sqrt{\varepsilon_0\mu_0}}P_{x\mathrm{L}}, \quad \bar{P}_{x\mathrm{NL}} = \frac{1}{\sqrt{\varepsilon_0\mu_0}}P_{x\mathrm{NL}},$$

$$\bar{E}_y = \sqrt{\frac{\varepsilon_0}{\mu_0}}E_y, \quad \bar{D}_y = \sqrt{\frac{1}{\varepsilon_0\mu_0}}D_y, \quad \bar{H}_x = H_x,$$

$$\bar{P}_{y\mathrm{L}} = \frac{1}{\sqrt{\varepsilon_0\mu_0}}P_{y\mathrm{L}}, \quad \bar{P}_{y\mathrm{NL}} = \frac{1}{\sqrt{\varepsilon_0\mu_0}}P_{y\mathrm{NL}},$$

$$\bar{S}_x = \frac{1}{\mu_0}S_x, \quad \bar{S}_y = \frac{1}{\mu_0}S_y, \quad \bar{\chi}_0^{(3)} = \chi_0^{(3)}\frac{\mu_0}{\varepsilon_0}.$$

Each time step was divided into four stages. The initial data for the iteration process are the values of E_x, D_x, E_y, and D_y on the nth discrete time step and H_y and H_x on the discrete time step $n = \frac{1}{2}$. At the first stage, Maxwell's equations are approximated, and we find from them, by using the known values of $\boldsymbol{E}$, $\boldsymbol{D}$, and $\boldsymbol{H}$, the values of $\boldsymbol{D}$ and $\boldsymbol{H}$ in the new time layers $n+1$ and $n+\frac{1}{2}$, respectively:

$$\begin{aligned}
\bar{H}_y\big|_{k+1/2}^{n+1/2} &= \bar{H}_y\big|_{k+1/2}^{n-1/2} - \frac{c\Delta t}{\Delta z}\left(\bar{E}_x\big|_{k+1}^{n} - \bar{E}_x\big|_{k}^{n}\right),\\
\bar{D}_x\big|_{k}^{n+1} &= \bar{D}_x\big|_{k}^{n} - \frac{c\Delta t}{\Delta z}\left(\bar{H}_y\big|_{k+1/2}^{n+1/2} - \bar{H}_y\big|_{k-1/2}^{n+1/2}\right),
\end{aligned} \tag{26}$$

$$\begin{aligned}
\bar{H}_x\big|_{k+1/2}^{n+1/2} &= \bar{H}_x\big|_{k+1/2}^{n-1/2} + \frac{c\Delta t}{\Delta z}\left(\bar{E}_y\big|_{k+1}^{n} - \bar{E}_y\big|_{k}^{n}\right),\\
\bar{D}_y\big|_{k}^{n+1} &= \bar{D}_y\big|_{k}^{n} + \frac{c\Delta t}{\Delta z}\left(\bar{H}_x\big|_{k+1/2}^{n+1/2} - \bar{H}_x\big|_{k-1/2}^{n+1/2}\right),
\end{aligned} \tag{27}$$

where $c = 1/\sqrt{\mu_0\varepsilon_o}$ is the speed of light in vacuum.

Before proceeding to the next sage, we consider difference schemes corresponding to Eqns (9) and (10). According to (9) and (10), the difference schemes corresponding to the linear response of a medium and allowing one to determine the values of $P_{ix\mathrm{L}}$ and $P_{iy\mathrm{L}}$ on the $n+1$th discrete time step can be represented in the form

$$\begin{aligned}
\bar{P}_{ix\mathrm{L}}\big|_{k}^{n+1} &= al_i\bar{P}_{ix\mathrm{L}}\big|_{k}^{n} - \bar{P}_{ix\mathrm{L}}\big|_{k}^{n-1} + cl_i\bar{E}_x\big|_{k}^{n},\\
\bar{P}_{iy\mathrm{L}}\big|_{k}^{n+1} &= al_i\bar{P}_{iy\mathrm{L}}\big|_{k}^{n} - \bar{P}_{iy\mathrm{L}}\big|_{k}^{n-1} + cl_i\bar{E}_y\big|_{k}^{n},
\end{aligned} \tag{28}$$

where $\bar{P}_{ix\mathrm{L}}\big|_{k}^{n-1}$, $\bar{P}_{ix\mathrm{L}}\big|_{k}^{n}$, $\bar{P}_{iy\mathrm{L}}\big|_{k}^{n-1}$, and $\bar{P}_{iy\mathrm{L}}\big|_{k}^{n}$ are linear polarisations of the medium on the $n-1$th and nth discrete time steps; $\bar{E}_x\big|_{k}^{n}$ and $\bar{E}_y\big|_{k}^{n}$ are the electric fields on the nth discrete time step; and

$$al_i = 2 - (\omega_i\Delta t)^2; \;\; cl_i = b_i(\omega_i\Delta t)^2. \tag{29}$$

At the second stage, the linear polarisations $\bar{P}_{ix\mathrm{L}}\big|_{k}^{n+1}$ and $\bar{P}_{iy\mathrm{L}}\big|_{k}^{n+1}$ of the medium are calculated from (28) at the $n+1$th discrete time step.

According to (22), the difference schemes corresponding to SRS in the medium and allowing one to determine the values of S_x and S_y on the $n+1$th discrete time step can be represented in the form

$$\begin{aligned}
\bar{S}_x\big|_{k}^{n+1} &= ar\bar{S}_x\big|_{k}^{n} + br\bar{S}_x\big|_{k}^{n-1} + cr\left(\bar{E}_x\big|_{k}^{n}\right)^2,\\
\bar{S}_y\big|_{k}^{n+1} &= ar\bar{S}_y\big|_{k}^{n} + br\bar{S}_y\big|_{k}^{n-1} + cr\left(\bar{E}_y\big|_{k}^{n}\right)^2,
\end{aligned} \tag{30}$$

where $\bar{S}_x\big|_{k}^{n-1}$, $\bar{S}_x\big|_{k}^{n}$, $\bar{S}_y\big|_{k}^{n-1}$, and $\bar{S}_y\big|_{k}^{n}$ are the values of functions on the $n-1$th and nth discrete time steps, respectively, and the quantities ar, br, and cr are determined by the expressions

$$ar = \frac{2 - (\omega_{\mathrm{R}}\Delta t)^2}{1 + \delta_{\mathrm{R}}\Delta t}, \quad br = \frac{1 - \delta_{\mathrm{R}}\Delta t}{1 + \delta_{\mathrm{R}}\Delta t}, \quad cr = \frac{\bar{\chi}_0^{(3)}(\omega_{\mathrm{R}}\Delta t)^2}{1 + \delta_{\mathrm{R}}\Delta t}. \tag{31}$$

At the third stage, the nonlinear polarisations $\bar{S}_x\big|_{k}^{n+1}$ and $\bar{S}_y\big|_{k}^{n+1}$ of the medium are calculated from (30) at the $n+1$th discrete time step.

According to (16) and (17), the Raman inertial nonlinear response $P_{x\mathrm{RNL}}$, $P_{y\mathrm{RNL}}$ of the medium at the $n+1$th discrete time step can be represented in the form

$$\begin{aligned}
\bar{P}_{x\mathrm{RNL}}\big|_{k}^{n+1} &= (1-\alpha)\bar{\chi}_0^{(3)}\bar{E}_x\big|_{k}^{n+1}\bar{S}_x\big|_{k}^{n+1}\\
&\quad + (1-\alpha)\bar{\chi}_0^{(3)}\bar{E}_x\big|_{k}^{n+1}\bar{S}_y\big|_{k}^{n+1},\\
\bar{P}_{y\mathrm{RNL}}\big|_{k}^{n+1} &= (1-\alpha)\bar{\chi}_0^{(3)}\bar{E}_y\big|_{k}^{n+1}\bar{S}_y\big|_{k}^{n+1}\\
&\quad + (1-\alpha)\bar{\chi}_0^{(3)}\bar{E}_y\big|_{k}^{n+1}\bar{S}_x\big|_{k}^{n+1}.
\end{aligned} \tag{32}$$

According to (15), the Kerr instant nonlinear response $P_{x\mathrm{KNL}}$, $P_{y\mathrm{KNL}}$ of the medium at the $n+1$th discrete time step has the form

$$\begin{aligned}
\bar{P}_{x\mathrm{KNL}}\big|_{k}^{n+1} &= \alpha\bar{\chi}_0^{(3)}\left(\bar{E}_x\big|_{k}^{n+1}\right)^3 + \alpha\bar{\chi}_0^{(3)}\bar{E}_x\big|_{k}^{n+1}\left(\bar{E}_y\big|_{k}^{n+1}\right)^2,\\
\bar{P}_{y\mathrm{KNL}}\big|_{k}^{n+1} &= \alpha\bar{\chi}_0^{(3)}\left(\bar{E}_y\big|_{k}^{n+1}\right)^3 + \alpha\bar{\chi}_0^{(3)}\bar{E}_y\big|_{k}^{n+1}\left(\bar{E}_x\big|_{k}^{n+1}\right)^2.
\end{aligned} \tag{33}$$

According to (24) and (25), the components D_x and D_y of the electric induction at the $n+1$th discrete time step can be written in the form

$$\bar{D}_x\big|_k^{n+1} = \bar{E}_x\big|_k^{n+1} + \sum_{i=1}^{3} \bar{P}_{ix\mathrm{L}}\big|_k^{n+1} + \bar{P}_{x\mathrm{KNL}}\big|_k^{n+1} + \bar{P}_{x\mathrm{RNL}}\big|_k^{n+1}, \tag{34}$$

$$\bar{D}_y\big|_k^{n+1} = \bar{E}_y\big|_k^{n+1} + \sum_{i=1}^{3} \bar{P}_{yx\mathrm{L}}\big|_k^{n+1} + \bar{P}_{y\mathrm{KNL}}\big|_k^{n+1} + \bar{P}_{y\mathrm{RNL}}\big|_k^{n+1}.$$

At the last stage, the fields $\bar{E}_x\big|_k^{n+1}$ and $\bar{E}_y\big|_k^{n+1}$ are determined from the given linear and nonlinear polarisations by using the recurrent expression

$$\bar{E}_x\big|_k^{p+1} = \bar{D}_x\big|_k^{n+1} - \sum_{i=1}^{3} \bar{P}_{ix\mathrm{L}}\big|_k^{n+1} \Big[1 + \alpha\bar{\chi}_0^{(3)}\big(\bar{E}_x\big|_k^{p}\big)^2 + \alpha\bar{\chi}_0^{(3)}\big(\bar{E}_y\big|_k^{p}\big)^2 + (1-\alpha)\bar{S}_x\big|_k^{n+1} + (1-\alpha)\bar{S}_y\big|_k^{n+1}\Big]^{-1},$$

$$\bar{E}_y\big|_k^{p+1} = \bar{D}_y\big|_k^{n+1} - \sum_{i=1}^{3} \bar{P}_{iy\mathrm{L}}\big|_k^{n+1} \Big[1 + \alpha\bar{\chi}_0^{(3)}\big(\bar{E}_y\big|_k^{p}\big)^2 + \alpha\bar{\chi}_0^{(3)}\big(\bar{E}_x\big|_k^{p}\big)^2 + (1-\alpha)\bar{S}_y\big|_k^{n+1} + (1-\alpha)\bar{S}_x\big|_k^{n+1}\Big]^{-1}, \tag{35}$$

where $\bar{E}_x\big|_k^{p} = \bar{E}_x\big|_k^{n+1}$ and $\bar{E}_y\big|_k^{p} = \bar{E}_y\big|_k^{n+1}$ are the electric fields at the beginning of iteration.

4. Results of numerical simulation and discussion

The numerical simulation was performed under the initial conditions

$$E_x(t, z=0) = E_{x0}\exp\left(-\frac{t^2}{\tau_0^2}\right)\cos\left[\frac{2\pi c}{\lambda_0}(t-\Delta t)\right],$$
$$E_y(t, z=0) = E_{y0}\exp\left(-\frac{t^2}{\tau_0^2}\right)\cos\left(\frac{2\pi c}{\lambda_0}t\right), \tag{36}$$

where E_{x0} and E_{y0} are the initial amplitudes of pulses with mutually orthogonal x- and y-polarisations.

The calculations were performed for the pulse duration $\tau_0 = 10$ fs and its central wavelength $\lambda_0 = 0.81$ μm. The amplitude of a pulse with the x-polarisation was $E_{x0} = 8.2 \times 10^9$ V m^{-1}, while for a pulse with the y-polarisation, the amplitudes $E_{y0} = 1.2 \times 10^9$, 2.6×10^9, 3.6×10^9, and 5.8×10^9 V m^{-1} were considered. The length of a medium for the give model was chosen to provide the coincidence of the network dispersion curve with the material dispersion curve [12]. The length of the medium used in calculations was $L = 525$ μm and the time delay Δt between the interacting pulses was varied from -20 to 40 fs.

Figure 1 presents the calculated dependences of the normalised power densities for orthogonally polarised pulses on the wavelength for different values of Δt and $E_{y0} = 5.8 \times 10^9$ V m^{-1}. The values of P_x and P_y were found from the expression

$$P_{x,y} = 10\lg\left(\frac{S_{x,y}}{S_{x0,y0}}\right) = 10\lg\left[\left|\int_{-\infty}^{\infty} E_{x,y}(t,z)\exp(\mathrm{j}2\pi\nu t)\mathrm{d}t\right|^2 \times \left|\int_{-\infty}^{\infty} E_{x,y}(t,z=0)\exp(\mathrm{j}2\pi\nu t)\mathrm{d}t\right|^{-2}\right]. \tag{37}$$

For comparison, the dashed curves in Fig. 1 show the power densities $E_x(t, z=0)$ and $E_y(t, z=0)$ for pulses incident on the medium.

Figure 2 shows the dependences of the shift of carrier frequencies of interacting pulses corresponding to the spectral maxima on the time delay between the pulses for different amplitudes E_{y0}. One can see that for -15 fs $> \Delta t >$ 15 fs, when the interaction of the pulses can be neglected, the carrier frequencies of pulses shift to the red due to self-action. This means that self-action of the

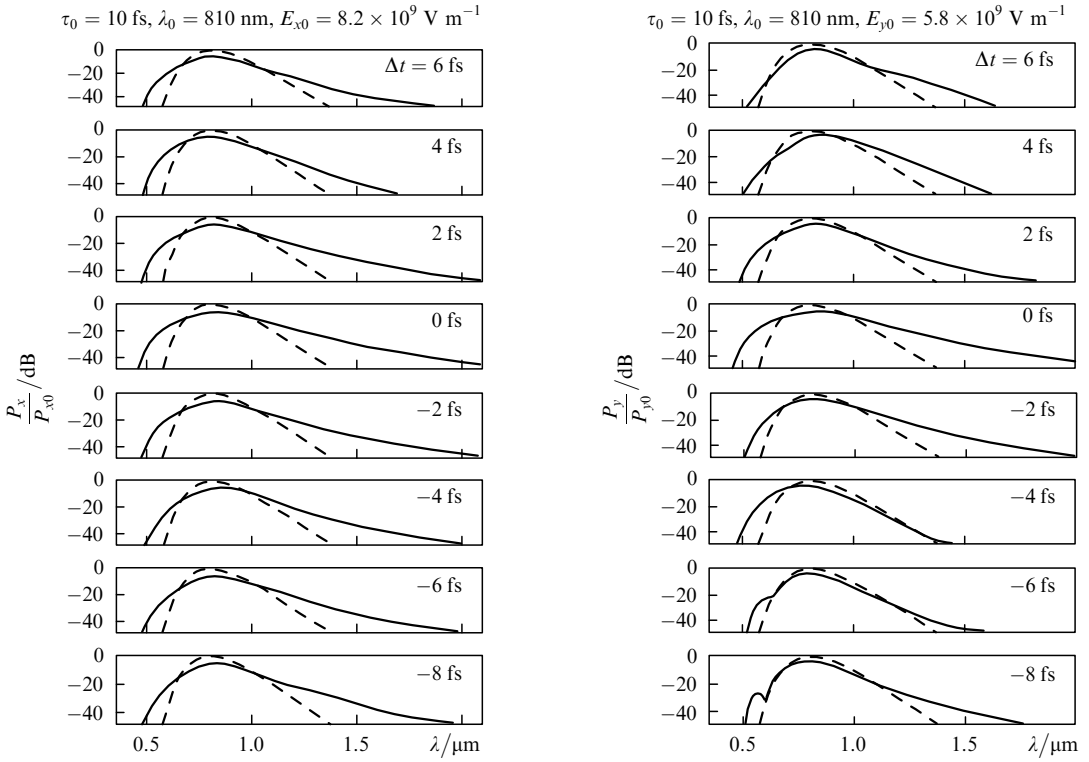

Figure 1.

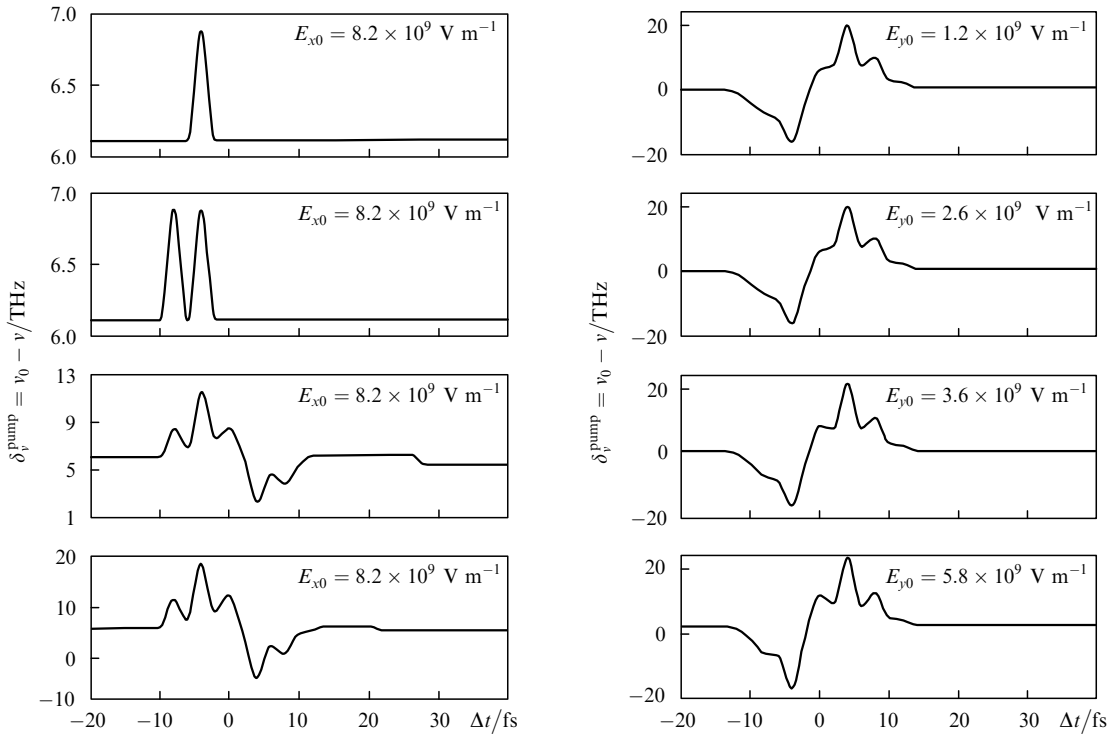

Figure 2.

pulses takes place, which is mainly related to the Raman inertial nonlinearity. As a result, the energy in the pulse spectrum is redistributed and the pulse spectrum shifts to the red. In particular, the carrier frequency $\nu_0 - \nu$ of the reference pulse E_x shifts by 6.1 THz, while the carrier frequency of the probe pulse E_y shifts by 2.3 THz for the initial field amplitude of 5.8×10^9 V m^{-1}. For smaller initial amplitudes of the probe field, the shift of the carrier frequency is zero.

It also follows from Fig. 2 that for $\Delta t < -1.5$ fs, when the reference pulse is delayed with respect to the probe pulse, the carrier frequency of the latter shifts to the blue. In this case, the maximum shift $\delta_{\nu\max}^{\rm probe} = \nu_0 - \nu_{\max}$ is -15.9 THz ($\Delta t = -3.85$ fs) for $E_{y0} = 1.2 \times 10^9$ V m^{-1}, -16 THz ($\Delta t = -4.12$ fs) for $E_{y0} = 2.6 \times 10^9$ V m^{-1}, -16 THz ($\Delta t = -3.92$ fs) for $E_{y0} = 3.6 \times 10^9$ V m^{-1}, and -16.75 THz ($\Delta t = -3.92$ fs) for $E_{y0} = 5.8 \times 10^9$ V m^{-1}. This means that, for the given time delays, the shift of the carrier frequency in the probe pulse spectrum is determined by the cross-action of the reference pulse on the probe pulse, caused by the Kerr inertialless nonlinearity, which is described by the second term $\alpha\varepsilon_0\chi_0^{(3)}E_y(t)E_x^2(t)$ in the right-hand side of equation (15b).

For $\Delta t \approx -1.5$ fs, the shift of the carrier frequency of the probe pulse caused by the cross-action of the reference pulse is zero.

In turn, for $\Delta t > -1.5$ fs, when the reference pulse begins to be ahead of the probe pulse, the carrier frequency of the latter shifts to the red. In this case, the maximum red shift $\delta_{\nu\max}^{\rm probe}$ is 19.85 THz ($\Delta t = 3.95$ fs) for $E_{y0} = 1.2 \times 10^9$ V m^{-1}, 19.85 THz ($\Delta t = 3.95$ fs) for $E_{y0} = 2.6 \times 10^9$ V m^{-1}, 21.32 THz ($\Delta t = 4.09$ fs) for $E_{y0} = 3.6 \times 10^9$ V m^{-1}, and 22.85 TH ($\Delta t = 4.09$ fs) for $E_{y0} = 5.8 \times 10^9$ V m^{-1}. This means that, for the given time delays, the carrier frequency of the probe pulse shifts due to the Raman cross-action of the reference pulse on the probe pulse. Namely, the excitation of molecular vibrations by the reference pulse leads to the energy redistribution in the probe pulse spectrum, resulting in the red shift of the carrier frequency of the probe pulse. In this case, the frequency shift is determined by the second term

$$\varepsilon_0(1-\alpha)\chi_0^{(3)}E_y(t)\int_{-\infty}^{t} g_{\rm R}(t-\tau)E_x^2(\tau){\rm d}\tau$$

in Eqn (16b).

As the input probe pulse amplitude is increased, both the Kerr inertialless self-action, determined by the first term $\alpha\varepsilon_0\chi_0^{(3)}E_y^3(t)$ in the right-hand side in Eqn (15b), and Raman inertial self-action, determined by the first term

$$\varepsilon_0(1-\alpha)\chi_0^{(3)}E_y(t)\int_{-\infty}^{t} g_{\rm R}(t-\tau)E_y^2(\tau){\rm d}\tau$$

in Eqn (16b), become substantial. Note at the same time that, as the input probe pulse amplitude is increased, the evolution of the reference pulse spectrum is determined not only by its self-action but also by the cross-action of the probe pulse. Indeed, one can see from Fig. 2 that for $E_{y0} = 3.6 \times 10^9$ and 5.8×10^9 V m^{-1}, the dependence of the carrier frequency shift of the reference pulse on the time delay becomes the mirror reflection of the dependence $\delta_\nu^{\rm probe}(\Delta t)$. In other words, the reference and probe pulses as if interchanged.

5. Conclusions

We have studied theoretically the cross-action of few-cycle laser pulses propagating in fused silica. The system of nonlinear Maxwell's equations was integrated numerically with respect to time by the finite difference method. Linearly polarised pulses with identical central frequencies

and mutually orthogonal polarisations have been considered. The calculations have been performed for a medium of length 525 μm. Both the instant Kerr inertialless response and the Raman response of the medium were taken into account in the nonlinear polarisation of the medium. The shift of the probe pulse spectrum caused by the cross-action of the reference pulse has been studied for different time delays between the interacting pulses and their spectra are calculated. The dependences of the spectra of interacting pulses on the time delay between them have been obtained.

The estimates presented in the paper show that the frequency shift of the probe pulse caused by the cross-action of the reference pulse at different time delays between the interacting pulses can be experimentally detected by using modern femtosecond lasers.

The results obtained in the paper can be used in the development of femtosecond optically controlled elements used in ultra high-speed optical communication systems.

References

1. Yan Y.X., Gamble E.B., Nelson K.A. *J. Chem. Phys.*,. **83**, 5391 (1985).
2. Ruhman S., Joly A.G., Nelson K.A. *IEEE J. Quantum Electron.*, **24**, 460 (1988).
3. Headley III C., Agrawal G.P. *J. Opt. Soc. Am. B*, **13**, 2170 (1996).
4. Gordon J.P. *Opt. Lett.*, **11**, 662 (1986).
5. Santhanam J., Agrawal G.P. *Opt. Commun.*, **222**, 413 (2003).
6. Hovhannisyan D.L., Stepanyan K.G. *J. Mod. Opt.*, **50**, 2201 (2003).
7. Kozlov S.A., Sazonov S.V. *Zh. Eksp. Teor. Fiz.*, **111**, 404 (1997).
8. Taflove A., Hagness S.C. *Computational Electrodynamics: the Finite-Difference Time-Domain Method* (Boston: Artech House, 2000).
9. Goorjian P.M., Taflove A., Joseph R.M., Hagness S.C. *IEEE J. Quantum Electron.*, **28**, 2416 (1992).
10. Ziolkowski R.W., Judkis J.B. *J. Opt. Soc. Am. B*, **10** (2), 186 (1993).
11. Joseph R.M., Taflove A. *IEEE Trans. Antennas and Propagation*, **45**, 364 (1997).
12. Serkin V.N., Shmidt E.M., Belyaeva T.L., Marti-Panameno E., Salazar H. *Kvantovaya Elektron.*, **24**, 923 (1997) [*Quantum Electron.*, **27**, 940 (1997)].
13. Fujii M., Tahara M., Sakagami I., Freude W., Russer P. *IEEE J. Quantum Electron.*, **40**, 175 (2004).
14. Nakamura S., Koyamada Y., Yoshida N., Karasawa N., Sone H., Ohtani M., Mizuta Y., Morita R., Shigekawa H., Yamashita M. *IEEE Photonic. Technol. Lett.*, **14**, 480 (2002).
15. Hovhannisyan D.L., Stepanyan K.G., Avagyan R.A. *J. Modern Opt.*, **52** (1), 97 (2005).
16. Hovhannisyan D.L., Stepanyan K.G., Avagyan R.A. *Opt. Commun.*, **245**, 443 (2005).
17. Agrawal G.P. *Nonlinear Fiber Optics* (New York: Academic Press, 1995).
18. Platonenko V.T., Khokhlov R.V. *Zh. Eksp. Teor. Fiz.*, **46**, 555 (1964).
19. Hovhannisyan, D.L., Manucharyan S.R. *Microwave Opt. Technol. Lett.*, **47** (4), 359 (2005).